

DRAG: Divergence-based Adaptive Aggregation in Federated learning on Non-IID Data

Feng Zhu, Jingjing Zhang, Shengyun Liu and Xin Wang

School of Information Science and Technology, Fudan University

School of Electronic, Information and Electrical Engineering, Shanghai Jiao Tong University

{20210720072, jingjingzhang, xwang11}@fudan.edu.cn

shengyun.liu@sjtu.edu.cn

Abstract

Local stochastic gradient descent (SGD) is a fundamental approach in achieving communication efficiency in Federated Learning (FL) by allowing individual workers to perform local updates. However, the presence of heterogeneous data distributions across working nodes causes each worker to update its local model towards a local optimum, leading to the phenomenon known as “client-drift” and resulting in slowed convergence. To address this issue, previous works have explored methods that either introduce communication overhead or suffer from unsteady performance. In this work, we introduce a novel metric called “degree of divergence,” quantifying the angle between the local gradient and the global reference direction. Leveraging this metric, we propose the divergence-based adaptive aggregation (DRAG) algorithm, which dynamically “drags” the received local updates toward the reference direction in each round without requiring extra communication overhead. Furthermore, we establish a rigorous convergence analysis for DRAG, proving its ability to achieve a sublinear convergence rate. Compelling experimental results are presented to illustrate DRAG’s superior performance compared to state-of-the-art algorithms in effectively managing the client-drift phenomenon. Additionally, DRAG exhibits remarkable resilience against certain Byzantine attacks. By securely sharing a small sample of the client’s data with the FL server, DRAG effectively counters these attacks, as demonstrated through comprehensive experiments.

Index Terms

Federated learning, local SGD, client-drift, byzantine attack.

I. INTRODUCTION

With the increasing complexity of machine learning tasks and the exponential growth in data volume, the adoption of distributed implementations, e.g., federated learning (FL), has been gaining considerable attention [1], [2], [3], [4]. The parameter-server (PS) setting stands as one of the most widely utilized paradigms in FL. In this approach, the PS broadcasts the latest global model to the workers for computation, while the workers, in turn, send their computed local models back to the PS for aggregation and update [5], [6], [7].

Due to the frequent bidirectional transmissions between the PS and the workers, communication efficiency has become a critical bottleneck in large-scale FL [8], [9]. To overcome this challenge, the local stochastic gradient descent (SGD) method [10], [11] has been introduced. This method enables each worker to perform multiple local updates before uploading the latest model, significantly enhancing communication efficiency. [11] proposes the widely-studied federated averaging (FedAvg) algorithm, where the communication frequency between the PS and the workers is increased, leading to improved performance. Under heterogeneous data distribution, FedAvg achieves remarkable performance compared to parallel SGD which does not employ local updates, which is also theoretically substantiated by rigorous convergence analysis [12], [13], [14], [15].

This paper focuses on FL with local SGD involving heterogeneous data. In particular, it aims to address the following two challenges:

Challenge 1: Client-Drift. The phenomenon of “client-drift” in local SGD is first identified in [16]. The authors observe that the local models of different workers tend to converge to local optima when dealing with heterogeneously distributed data. Consequently, the straightforward averaging of these local models results in poor convergence outcomes. State-of-the-art algorithms such as SCAFFOLD [17] and AdaBest [18] that utilize control variates to mitigate client-drift usually have unsteady performance and cannot adapt to diverse settings.

To address this issue, we propose a method named divergence-based adaptive aggregation (DRAG). The proposed DRAG algorithm introduces a novel metric named “degree of divergence”, which quantifies the extent of the local update of each worker in each round diverging from the reference direction. The reference direction, having a momentum form, is a weighted sum of all the historical global update directions. Leveraging the newly defined metric, the local update of each worker is then dynamically “dragged” toward the reference direction through weighted vector manipulation. The PS finally aggregates the dragged local updates to update the global model. This approach can effectively mitigate the client-drift phenomenon while preserving the diversity of local gradients and accelerates the convergence process in distributed learning scenarios with heterogeneous data distributions.

Challenge 2: Byzantine attack. As FL operates in a distributed manner, it is susceptible to adversarial attacks launched by malicious clients, commonly known as Byzantine attacks [19], [20], [21]. For instance, one type of Byzantine attack involves the malicious client reversing the direction of the local update or scaling the local gradient by a factor to negatively influence the training process [22]. In this work, the proposed DRAG method is proven to be effective in mitigating this type of attack through vector manipulation, ensuring the integrity and security of the FL process even in the presence of malicious clients.

Our contributions: Motivated by these challenges, we investigate a PS-based framework under heterogeneous data distribution. The main contribution can be summarized as follows.

- We introduce a new metric called “degree of divergence” that utilizes the angle to quantify the deviation between workers’ local updates and the weighted sum of historical global updates. This metric forms the basis for our proposed method, divergence-based adaptive aggregation (DRAG), effectively addressing the client-drift phenomenon and accelerating the convergence rate.
- We establish a rigorous convergence analysis of the DRAG algorithm, demonstrating that it achieves a sublinear convergence rate similar to other local SGD methods.
- The performance of DRAG is evaluated on EMNIST and CIFAR-10 datasets, and we conduct a comprehensive comparison with state-of-the-art algorithms, revealing that our method consistently achieves superior results.
- Finally, we demonstrate that DRAG exhibits resilience against certain Byzantine attacks, such as reversing the local update direction or scaling the local update.

II. RELATED WORKS

In this section, we provide a brief review of prior research on strategies employed to address the client-drift issue resulting from data heterogeneity. Furthermore, we offer background information on byzantine attacks.

[16] initiates a series of research attempting to deal with the so-called “client-drift” issue. There are several categories of methods used to address client-drift in FL. One is to incorporate the idea of variance reduction [23], [24] into local SGD such as [25], [26], [27], [28]. However, these methods often require the full participation of workers, making them less practical when only a subset of devices are active.

Another category involves using control variates to compensate for the drift. [17] proposes SCAFFOLD that uses local and global control variates to correct the drift on the client side. Building on SCAFFOLD, [29] further adopts the idea of momentum to for server-level optimization. Additionally, employing local and global variates, FedDyn [30] and AdaBest [18] correct the drift on both the server and client sides where Adabest did not use historical information for the global variate, unlike FedDyn.

Another effective approach to reduce client-drift is through explicit gradient constraint. FedProx, introduced in [31], adds a regularization term in the objective function to prevent the drift from being too far. Decoupling the local and global model, [32] utilizes both control variates and regularization terms to jointly learn the gap between the local model and the global one.

Next, we provide a brief overview of byzantine attacks in the context of FL. Due to the distributed nature of FL, it becomes vulnerable to attacks if some of the clients experience software bugs or fall under the control of malicious entities. These attacks, widely known as byzantine attacks [19], [20], [22], can potentially compromise the integrity of the learning process and the security of the overall system. It is essential to develop defense mechanisms to counter such attacks and ensure the robustness and reliability of federated learning in the presence of adversarial clients.

Apart from the reversing direction attack mentioned in the introduction part, there are other more advanced attacks in the literature, which we briefly introduce as follows. The Label flipping attack is simple to implement: In supervised learning, the malicious client flips the labels of its training examples in a reverse way, or any other way that induces a mismatch between the data example and its label [33]. Krum attack [34] and Trim attack [33] are coupled with their corresponding gradient aggregation rules.

One of the approaches to defending against byzantine attacks is to remove the outliers in the clients through utilizing byzantine-robust aggregation rules, i.e., comparing the local updates of the clients and getting rid of the anomalies [34], [33], [35]. For instance, the Krum aggregation rule [34] uses the one local update that has the smallest Euclidean distance to the rest of the clients to update the global model. However, this kind of method loses its robustness against byzantine attacks when malicious clients take up a large proportion since it lacks *root of trust*. To tackle this problem, [20] proposes the FLTrust algorithm where the server maintains a small subset of the correct dataset named the “*root dataset*”. By doing this, the server then achieves a trusted source of each global update direction and improves its robustness against attacks.

The rest of the paper is organized as follows. Section III describes the system model. The development of the proposed DRAG scheme is delineated in Section IV. Section V presents the convergence analysis of DRAG. Numerical results are provided in Section VI. Section VII concludes the work.

III. SYSTEM MODEL

In this paper, we investigate an FL architecture consisting of M workers denoted by the set $\mathcal{M} := \{1, \dots, M\}$. Each worker m maintains a local dataset \mathcal{D}_m with a size of N_m . These datasets are drawn from a global dataset $\mathcal{D} = \{z_i\}_{i=1}^N$, i.e., we have

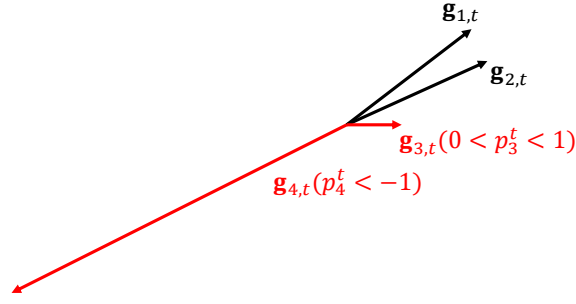


Fig. 1. Illustration of byzantine attacks dealt with in this work, where the black color represents the normal clients and the red color represents the malicious ones.

$\mathcal{D} = \bigcup_{m \in \mathcal{M}} \mathcal{D}_m$. The objective is to solve the minimization problem, where the objective function is defined as the average sum of local functions contributed by individual workers:

$$\begin{aligned} \min_{\theta \in \mathbb{R}^d} f(\theta) &= \frac{1}{M} \sum_{m \in \mathcal{M}} F_m(\theta), \\ \text{with } F_m(\theta) &:= \mathbb{E}[F_m(\theta; z_m)], m \in \mathcal{M}, \end{aligned} \quad (1)$$

where parameter θ with dimension d is the variable to be optimized and $\{F_m(\theta), m \in \mathcal{M}\}$ are smooth functions, and z_m is a sample randomly selected from the local dataset \mathcal{D}_m of worker m .

With the objective function defined in (1), we attempt to solve the problem in an iterative manner with local SGD. In particular, at each training round j , the PS broadcasts the latest global model θ^t to a subset \mathcal{S}^t of S randomly selected workers. Then each worker m sets its local model $\theta_m^{t,0} = \theta^t$ and performs U local updates via the following formula

$$\theta_m^{t,u+1} = \theta_m^{t,u} - \frac{\eta}{B} \sum_{b=1}^B \nabla F(\theta_m^{t,u}; z_{m,b}^{t,u}), \quad (2)$$

for local iteration $u = 0, \dots, U - 1$. Note that η is the stepsize; B is the mini-batch size; $\frac{1}{B} \sum_{b=1}^B \nabla F(\theta_m^{t,u}; z_{m,b}^{t,u})$ is the mini-batch gradient to be computed by worker m at iteration u and $z_{m,b}^{t,u}$ are drawn independently from dataset \mathcal{D}_m across all workers, batches, local iterations and training rounds. Each worker m then sends \mathbf{g}_m^t to the server. The variable \mathbf{g}_m^t represents the discrepancy between the latest local model after U local updates and the original global model received at the beginning of the training round t . Specifically, for each worker m in training round t , we define \mathbf{g}_m^t as

$$\mathbf{g}_m^t = \theta_m^{t,U} - \theta^t. \quad (3)$$

Lastly, the PS aggregates the local models to update the global model:

$$\theta^{t+1} = \theta^t + \frac{1}{S} \sum_{m \in \mathcal{S}^t} \mathbf{g}_m^t. \quad (4)$$

The training process continues some convergence criterion is satisfied.

We proceed to elaborate on the scenario with the byzantine attack that we aim to defend against in this work. In the randomly selected subset \mathcal{S}^t , we assume the presence of A malicious clients denoted by $\mathcal{A}^t \in \mathcal{S}^t$. As shown in Fig. 1, during each training round t , after completing U local updates, each malicious client $m \in \mathcal{A}^t$ manipulates their local model update $\theta_m^{t,U} - \theta^t$ by multiplying it with a scalar p_m^t , denote as $\hat{\mathbf{g}}_m^t = p_m^t(\theta_m^{t,U} - \theta^t)$. Note that p_m^t can be either positive or negative. Subsequently, the modified update $\hat{\mathbf{g}}_m^t$ is sent to the server, effectively reversing the update direction or scaling the magnitude of the update. The PS then aggregates the received local models as follows: Lastly, the PS aggregates the local models to update the global model:

$$\theta^{t+1} = \theta^t + \frac{1}{S} \left(\sum_{m \in \mathcal{A}^t} \hat{\mathbf{g}}_m^t + \sum_{m \in \mathcal{S}^t \setminus \mathcal{A}^t} \mathbf{g}_m^t \right). \quad (5)$$

IV. DIVERGENCE-BASED ADAPTIVE AGGREGATION (DRAG) ALGORITHM

In this section, we introduce the proposed divergence-based adaptive aggregation (DRAG) method. In contrast to most state-of-the-art algorithms designed to tackle client drift by employing control variates for local and global model alignment, the proposed DRAG method adopts a heuristic and intuitive manner that “drags” each local model toward the reference direction through vector manipulation, with the extent of dragging determined by a metric we define as the “degree of divergence”. To establish the theoretical feasibility of DRAG, we conduct a rigorous convergence analysis that provides compelling evidence of its convergence properties.

A. Definitions

To commence, we define two crucial new variables: the reference direction and the degree of divergence. These variables play a key role in the process of dragging the local gradient.

1) *Reference Direction*: The objective of the reference direction \mathbf{r}^t is to offer a practical and sensible direction for modifying the local gradients, thereby facilitating the formation of an enhanced global update direction. Particularly, the updating formula for the reference direction is given as:

$$\mathbf{r}^t = \begin{cases} (1 - \alpha)\mathbf{r}^{t-1} + \alpha\Delta^{t-1}, & \text{for } t \geq 1 \\ \frac{1}{S} \sum_{m \in \mathcal{S}^t} \mathbf{g}_m^t, & \text{for } t = 0. \end{cases} \quad (6)$$

To rewrite it as a closed-form expression, we have:

$$\mathbf{r}^t = \frac{(1 - \alpha)^t}{S} \sum_{m \in \mathcal{S}^t} \mathbf{g}_m^t + \sum_{i=0}^{t-1} \alpha(1 - \alpha)^{t-i-1} \Delta^i, \quad t \geq 1. \quad (7)$$

Here $\alpha \in (0, 1)$ is some constant to control the weights of the historical directions. Furthermore, Δ^t is the aggregated modified gradients at the PS and can be calculated as

$$\Delta^t = \frac{1}{S} \sum_{m \in \mathcal{S}^t} \mathbf{v}_m^t, \quad (8)$$

with \mathbf{v}_m^t being the modified local gradient defined below.

The expression clearly demonstrates that the reference direction has a momentum form which is a weighted sum of all the historical global gradients Δ^i , for $i = 0, 1, \dots, t$. Significantly, the weights assigned to the most recent global updates progressively increase as α grows larger. When α is set to 1, the reference direction becomes equivalent to the previous global gradient Δ^{t-1} . Notably, the hyper-parameter α can be adjusted to fit different practical scenarios.

2) *Degree of Divergence*: The degree of divergence represents a fundamental aspect of the DRAG algorithm. This metric serves a critical role in measuring the extent to which the local update \mathbf{g}_m^t of each worker m in each training round t diverges from the reference direction \mathbf{r}^t .

The degree of divergence is quantified by utilizing the angle \angle_m^t between the local gradient \mathbf{g}_m^t and the reference direction \mathbf{r}^t , given as

$$\angle_m^t = \arccos \frac{\langle \mathbf{g}_m^t, \mathbf{r}^t \rangle}{\|\mathbf{g}_m^t\| \|\mathbf{r}^t\|}. \quad (9)$$

By dividing \angle_m^t over $\pi/2$, and approximating the arccos function with a linear function $y = -\frac{\pi}{2}x + \frac{\pi}{2}$ (this is one of many choices, one may also use $y = -x + \pi/2$), we define the metric of degree of divergence λ_m^t as

$$\lambda_m^t =: c \left(1 - \frac{\langle \mathbf{g}_m^t, \mathbf{r}^t \rangle}{\|\mathbf{g}_m^t\| \|\mathbf{r}^t\|} \right) \in [0, 2c], \quad (10)$$

where the constant $c \in [0, 1]$ is a hyper-parameter, providing the flexibility to manually adjust the metric to suit various settings. It is worth noting that λ_m^t is adaptable for each worker m at each round t , with a larger value of λ_m^t indicating a more significant divergence between the local gradient \mathbf{g}_m^t and the reference direction \mathbf{r}^t .

3) *Vector Manipulation*: Utilizing the predefined reference direction \mathbf{r}^t and the degree of divergence λ_m^t , we propose to drag each local gradient \mathbf{g}_m^t towards the reference direction based on its degree of divergence through vector manipulation. This process yields the modified local gradient \mathbf{v}_m^t , given as

$$\mathbf{v}_m^t = (1 - \lambda_m^t)\mathbf{g}_m^t + \frac{\lambda_m^t \|\mathbf{g}_m^t\|}{\|\mathbf{r}^t\|} \mathbf{r}^t. \quad (11)$$

Note that the modified gradient \mathbf{v}_m^t is a weighted sum of the original local gradient \mathbf{g}_m^t and the normalized reference direction $\frac{\|\mathbf{g}_m^t\|}{\|\mathbf{r}^t\|} \mathbf{r}^t$, with the weights being $1 - \lambda_m^t$ and λ_m^t , respectively. By adaptively tuning the hyper-parameter c , we can effectively

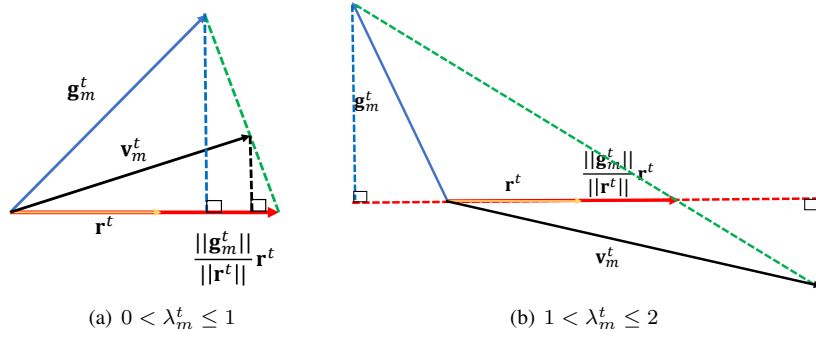


Fig. 2. Illustration of vector manipulation of DRAG. It is clear that the modified gradient \mathbf{v}_m^t (solid black line) has a larger component on the reference direction \mathbf{r}^t (solid yellow line) than the original one \mathbf{g}_m^t (solid blue line).

reduce the client drift while preserving the diversity of the local gradients. Additionally, the reference direction \mathbf{r}^t is normalized to match the norm of \mathbf{g}_m^t , ensuring that the modified gradient \mathbf{v}_m^t consistently has a greater component aligned with \mathbf{r}^t compared to the original gradient \mathbf{g}_m^t .

Remark 1. While the existing methods [31] generally utilize the norms of the local gradients to quantify the degree of similarity of the local functions, they may not be suitable for handling heterogeneous data distributions, as the local gradients often diverge from the global gradient. Thus, we propose a more appropriate and reasonable metric to quantify the dissimilarity in such scenarios.

Remark 2. An illustration demonstrating how the degree of divergence λ_m^t and the reference direction \mathbf{r}^t can be utilized to guide the local gradient is provided in Fig. 2. Specifically, using the vector manipulation operation, when $0 < \lambda_m^t \leq 1$, the resulting \mathbf{v}_m^t effectively mitigates the drift while preserving the diversity of each local gradient. Conversely, when $1 < \lambda_m^t \leq 2$, indicating that the local gradient diverges in the opposite direction to the reference direction, the \mathbf{g}_m^t component is reversed according to (11) to ensure adherence to the correct update direction.

B. Algorithm Description

With the above definitions, we proceed to present the details of the proposed algorithm, consisting of three steps in each training round.

Step 1: At each training round t , the PS first broadcasts the current global parameter θ^t to the workers in a random selected set \mathcal{S}^t .

Step 2: Each worker in \mathcal{S}^t then performs U local updates via (2) and sends its the difference $\mathbf{g}_m^t = \theta_m^{t,U} - \theta^t$ back to the PS.

Step 3: The PS first calculates the reference direction \mathbf{r}^t via (7) and the degree of divergence λ_m^t via (10). With these two variables, the PS then drags each \mathbf{g}_m^t towards the reference direction \mathbf{r}^t via (11), yielding the modified gradient \mathbf{v}_m^t . In the end, the PS aggregates the modified gradients with $\Delta^t =: \frac{1}{S} \sum_{m \in \mathcal{S}^t} \mathbf{v}_m^t$ and updates the global model with $\theta^{t+1} = \theta^t - \Delta^t$.

Usefulness of the degree of divergence. As illustrated in Fig. 2, it can be seen that the modified gradient \mathbf{v}_m^t substantially reduces client drift while concurrently preserving the diversity of gradients. This is achieved by increasing the component aligned with the reference direction while maintaining the component in the original direction.

To summarize the DRAG algorithm, it stands apart from control-variates-based methods by offering an intuitive geometric explanation. By adaptively dragging the local gradient towards the reference direction based on each worker's degree of divergence, the algorithm incorporates momentum and provides valuable insights for the desired update direction. The vector manipulation effectively tackles the client drift issue while preventing excessive correction of local gradients, thereby preserving their diversity. Both the reference direction and the degree of divergence include hyper-parameters that enable adaptation to different practical scenarios.

C. Defending Against byzantine Attacks

In this subsection, we illustrate the essential adaptations made to the DRAG algorithm to ensure its robustness against byzantine attacks. These attacks involve malicious clients attempting to reverse the gradient direction or scale its module. By incorporating specific modifications, DRAG is fortified to handle such adversarial behavior while maintaining the accuracy and security of the federated learning process.

The malicious effects of attackers can undermine the usefulness of the reference direction formed by the weighted sum of all the historical global update directions as guidance for the training process. Therefore, to defend against the attacks, the key improvements are the selection of the reference direction \mathbf{r}^t and the modified gradient \mathbf{v}_m^t .

Reference direction: The server is required to maintain a small root dataset $\mathcal{D}_{root} \in \mathcal{D}$ as in [20]. At each round t , the PS also updates a copy of the current global model θ^t using the root dataset \mathcal{D}_{root} for U local iterations and arrives at the updated global model $\theta^{t,U}$, i.e.,

$$\theta^{t,u+1} = \theta^{t,u} - \frac{\eta}{B} \sum_{b=1}^B \nabla F(\theta^{t,u}; z_b^{t,u}), \quad (12)$$

for $u = 0, \dots, U - 1$, where we have $\theta^{t,0} = \theta^t$ and $z_b^{t,u}$ is drawn independently from dataset \mathcal{D}_{root} across all batches, local iterations and training rounds. The reference direction \mathbf{r}^t is then set as

$$\mathbf{r}^t =: \theta^{t,U} - \theta^t. \quad (13)$$

Vector manipulation: Since the malicious client might scale the module of the local gradient, we can no longer use (11) as the vector manipulation formula because the module of the resulted \mathbf{v}_m^t would be abnormally large or small. Instead, we normalize the module of each local gradient \mathbf{g}_m^t according to the trusted reference direction \mathbf{r}^t in (13) to defend against the module scaling attack, i.e.,

$$\mathbf{v}_m^t := (1 - \lambda_m^t) \frac{\|\mathbf{r}^t\|}{\|\mathbf{g}_m^t\|} \mathbf{g}_m^t + \lambda_m^t \mathbf{r}^t. \quad (14)$$

The algorithm operates the same as the scenario without attacks (see Section IV B) with the above variables.

Remark 3. With the reference direction obtained from a trusted source, which provides a general update direction for the training process, and the module normalization operation, the modified DRAG can effectively address the Byzantine attack mentioned in Section III. To counter the attack that scales the magnitude of the local gradient, we employ normalization on each gradient to prevent any anomaly in the magnitude. As for the attack that reverses the direction, with (14), DRAG can automatically correct it by reversing the gradient back if $1 - \lambda_m^t < 0$, signifying excessive divergence from the reference direction (with the value of c appropriately chosen), which is also illustrated in Fig. 2.

V. CONVERGENCE ANALYSIS OF DRAG

In this section, we rigorously establish the convergence rate of DRAG for non-convex objective functions, which are prevalent in many machine learning tasks. We start by introducing two assumptions that are utilized in the analysis, as stated below.

Assumption 1 (Smoothness and Lower Boundedness) *Each local function $F_m(\theta)$ is L -smooth, i.e.,*

$$\|\nabla F_m(\theta_1) - \nabla F_m(\theta_2)\| \leq L \|\theta_1 - \theta_2\|, \quad (15)$$

$\forall \theta_1, \theta_2 \in \mathbb{R}^d$. The objective function F is also assumed to be lower-bounded by F^* .

Assumption 1 is the most common assumption used in convergence analysis, as in [36] [36], [12], [15].

Assumption 2 (Unbiasedness and Bounded Variance) *For the given model parameter θ , the local gradient estimator is unbiased, i.e.,*

$$\mathbb{E}[\nabla F_m(\theta; z)] = \nabla F_m(\theta). \quad (16)$$

Moreover, both the variance of the local gradient estimator and that of the local gradient from the global one are bounded, i.e., there exist two constants $\sigma_L, \sigma_G > 0$, such that

$$\mathbb{E}[\|\nabla F_m(\theta; z) - \nabla F_m(\theta)\|^2] \leq \sigma_L^2, \forall m \quad (17)$$

$$\mathbb{E}[\|\nabla F_m(\theta) - \nabla f(\theta)\|^2] \leq \sigma_G^2, \forall m. \quad (18)$$

Assumption 2 is also widely adopted when considering data heterogeneity, such as in [36], [37], [38].

The above assumptions are sufficient to arrive at the following theorem, which is the upper bound for the expectation of the average squared gradient norm $\frac{1}{T} \mathbb{E} \left[\sum_{t=0}^{T-1} \|\nabla f(\theta^t)\|^2 \right]$.

Theorem 1 *Under Assumption 1 and 2, by choosing a stepsize η satisfying $\eta \leq \frac{1}{8LU}$, there exists a positive constant $\gamma < \frac{1-3c}{2} - \left(5c + \frac{\eta LU}{2}\right) (90U^2 L^2 \eta^2 + 3) - 15(1-c)L^2 U^2 \eta^2$, such that*

$$\frac{1}{T} \sum_{t=0}^{T-1} \|\nabla f(\theta^t)\|^2 \leq \frac{f(\theta^0) - f^*}{\gamma \eta UT} + V, \quad (19)$$

where $V = \frac{1}{\gamma} \left[\frac{4c\sigma_L^2}{BU} + \frac{\eta\sigma_L^2 L}{2B} + \left(\frac{5c}{U} + \frac{\eta L}{2}\right) (15U^2 L^2 \eta^2 V_1 + 3U\sigma_G^2) + \frac{5(1-c)L^2 \eta^2}{2} V_1 \right]$ and $V_1 = \sigma_L^2 + 6U\sigma_G^2$.

Theorem 1 clearly states that provided the objective function is L -smooth and the global and local variances of the gradients are bounded, the proposed DRAG can then finally converge at a sublinear speed. Further, by selecting a stepsize η with the form $\mathcal{O}(1/\sqrt{T})$, we can readily achieve a convergence rate of the level $\mathcal{O}(1/\sqrt{T})$.

VI. SIMULATION RESULTS

In this section, we demonstrate the advantages of the DRAG algorithm by conducting a comprehensive performance comparison against state-of-the-art algorithms, including SCAFFOLD [17], AdaBest [18], FedProx [31], and the vanilla FedAvg [11]. Our evaluation is carried out on both the EMNIST dataset and the CIFAR-10 dataset, with scenarios of both partial and full worker participation. Additionally, we assess the robustness of the algorithms against byzantine attacks on these two datasets.

A. Setting Up

EMNIST Dataset. The EMNIST dataset [39] is an extended version of the famous MNIST dataset. Besides the handwritten digits from the MNIST dataset, the EMNIST dataset also includes handwritten letters. There are in total six different splits in the dataset and we used the “balanced” data split in this work with 47 balanced classes of data. Each piece of data is a 28×28 grey image and there are 131,600 characters in the 47 balanced classes.

CIFAR-10 Dataset. The CIFAR-10 dataset [40] is composed of 60000 32×32 color images in a total of 10 classes, with 6000 images in each class. There are 50000 images for training and 10000 for testing. Since it is a color image dataset, it is supposed to be more challenging than the EMNIST dataset.

Byzantine Attack. We set a total of $M = S = 10$ clients and the dataset used here is the CIFAR-10 dataset. The byzantine attack initiated by the malicious client is as described in Section III. To be specific, the scalar p_m^t conforms to normal distribution with zero mean and the variance is $\sigma^2 = 3$. The DRAG is also modified according to Section IV-C, with the root dataset maintaining $N_{root} = 3000$ pieces of data samples drawn randomly from the global dataset.

Data Heterogeneity. As in [20], we define the heterogeneity of data as follows. Any training data with label ℓ is assigned to client $\ell \bmod M$ with probability q and to any other client with probability $\frac{1-q}{M-1}$. In dealing with client-drift, the high heterogeneous data distribution is implemented by setting $q = 1$. In countering the byzantine attack, we define low data heterogeneity as $q = \frac{1}{M}$ and high data heterogeneity as $q = 1$.

B. Performance Analysis

Fig. 3(a) and (b) plot the performance comparison of different algorithms under the EMNIST dataset ($q = 1$), with full and partial worker participation, respectively. To be specific, there are in total $M = 40$ workers and $S = 10$ for partial worker participation. Each worker performs $U = 5$ local updates. All the algorithms stop updating once the test accuracy reaches 80%. The stepsize η is 0.1. We used a two-layer fully connected network with 500 hidden units. The hyperparameters of the algorithms are listed below. For AdaBest, $\mu = 0.02, \beta = 0.8$; for DRAG, $c = 0.25, \alpha = 0.6$ for partial participation and $\alpha = 1$ for full participation; $\mu = 0.2$ for FedProx.

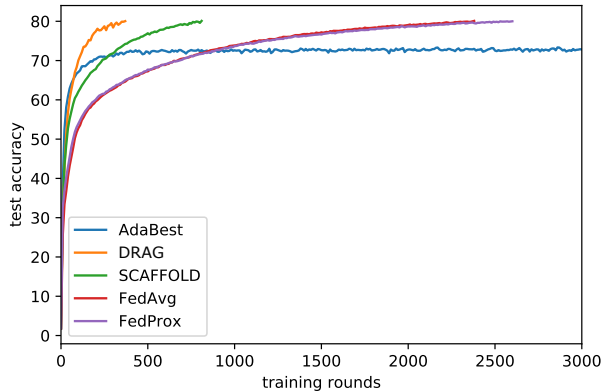
The comparison of different methods highlights the importance of addressing the client-drift issue. FedAvg and FedProx demonstrate subpar performance when neglecting this concern. While AdaBest is effective, it lacks robustness concerning the number of participating clients. Scaffold maintains relatively good performance in both cases, benefiting from its use of control variates to correct for client-drift in local updates. However, our proposed method, DRAG, exhibits significant superiority, especially in the presence of full participation. This advantage is attributed to the momentum-based reference direction, which provides a more accurate training direction, and the vector manipulation operation, which contributes to effective alignment with the reference direction.

In Fig. 4, we test the performances of these algorithms on the CIFAR-10 dataset ($q = 1$) with $M = 20$ workers for full participation and $S = 5$ workers for partial participation. Each worker performs $U = 5$ local updates. All the algorithms stop updating once the test accuracy reaches 70%. The stepsize η is 0.1. We used a CNN with two convolution layers and three fully-connected layers. For AdaBest, $\mu = 0.02, \beta = 0.2$; for DRAG, $c = 0.1, \alpha = 0.2$ for partial participation and $\alpha = 1$ for full participation; $\mu = 0.2$ for FedProx.

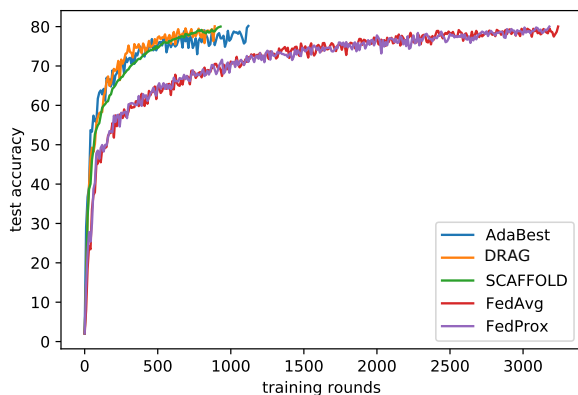
In this setting, AdaBest still performs relatively better with partial participation; however, SCAFFOLD and FedProx show limited improvement compared to FedAvg, as previously observed in [41]. On the other hand, DRAG outperforms all other algorithms significantly. Specifically, it achieves 70% test accuracy with only half of the training rounds compared to FedAvg with partial participation, and this proportion further reduces to 1/4 under full participation.

To summarize, DRAG consistently outperforms other algorithms in handling client drift across various settings. Its success can be attributed to its heuristic and intuitive design, which avoids using control variates or regularization terms. Instead, DRAG leverages tunable hyper-parameters c and α to balance the weights of the local gradient direction and the reference direction, respectively. This adaptability enables DRAG to develop a more accurate reference direction, further contributing to its superior performance.

Fig. 5 presents the performance of DRAG, FLTrust [20], and FedAvg under byzantine attacks with low data heterogeneity ($q = \frac{1}{M}$), and there is $A = 1$ attacker among the $M = S = 10$ clients. In the plot, FedAvg’s performance declines rapidly due to its lack of counter-attack techniques. In contrast, FLTrust demonstrates convergence by utilizing a small data sharing (root dataset) and ReLU-clipped cosine similarity. However, DRAG exhibits greater stability than FLTrust with just one data sharing step. The key advantage of DRAG lies in its ability to preserve the attacker’s useful information through scaling and



(a) full participation



(b) partial participation

Fig. 3. Performance comparison of DRAG with state-of-the-art algorithms under the EMNIST dataset with full and partial worker participation.

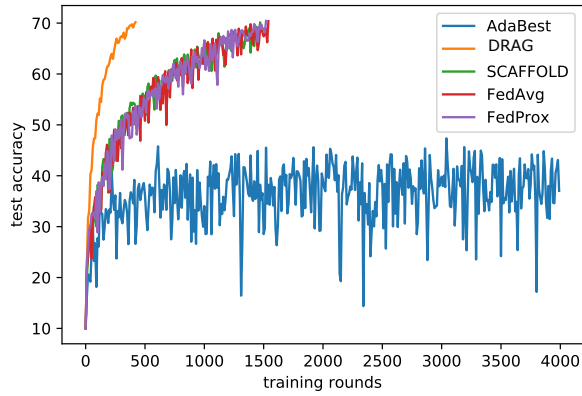
vector manipulation, instead of entirely removing the attacker. This property enables DRAG to achieve superior performance in handling byzantine attacks while maintaining the integrity of the FL process.

In Fig. 6, we increase the heterogeneity of data distribution among clients by setting $q = 1$. Under this setting, the performance of FedAvg is still degraded as expected while FLTrust cannot converge at all. This is primarily due to the ReLU-clipping operation in FLTrust. As the heterogeneity of data increases, it is common that the local model update of a normal client diverges significantly from the trusted root direction. However, in FLTrust, such normal clients are erroneously identified as malicious and removed, causing the training process to crash. As analyzed above, DRAG retains its superiority even with the increased data heterogeneity.

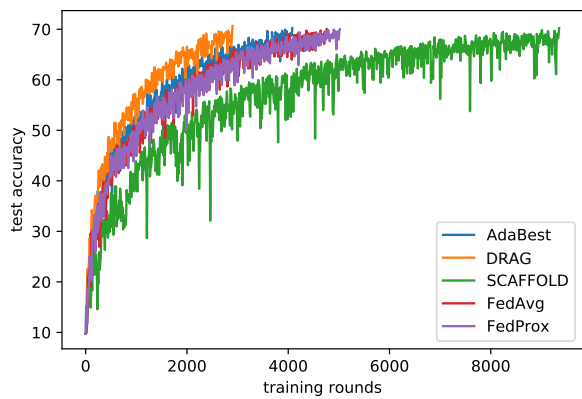
To further substantiate the effectiveness of DRAG in handling byzantine attacks, we conduct performance testing on EMNIST, as shown in Fig.7 and Fig.8. In this setting, we increase the number of attackers to $A = 4$ among a total of $M = 10$ clients, as EMNIST is less challenging compared to CIFAR-10. We observe that FedAvg also achieves decent performance under low data heterogeneity since the malicious gradients are diluted through averaging, leading to a less negative impact on the training process compared to using CIFAR-10. Similarly, FLTrust performs well under low data heterogeneity, but the performance is limited when data is highly heterogeneously distributed, as it tends to mistake good clients for malicious ones. In contrast, DRAG consistently maintained its superiority across different data heterogeneity levels.

VII. CONCLUSION

In this work, we introduce a novel scheme named divergence-based adaptive aggregation (DRAG) to address the client-drift issue in heterogeneous data distribution with local SGD. Unlike methods that rely on control variates or regularization terms, DRAG employs a heuristic approach, dynamically dragging each local gradient towards the reference direction based on the degree of divergence. We provide rigorous convergence analysis to theoretically support the feasibility of DRAG.



(a) full participation



(b) partial participation

Fig. 4. Performance comparison of DRAG with state-of-the-art algorithms under the CIFAR-10 dataset with full and partial worker participation.

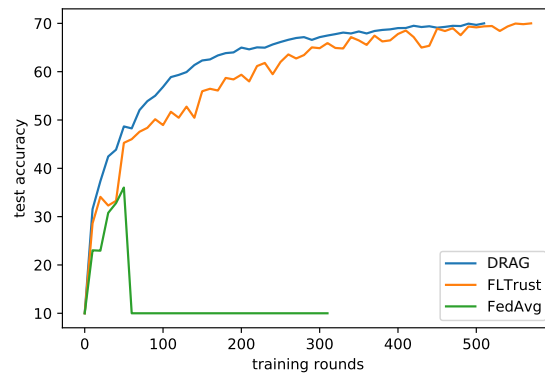


Fig. 5. Performance comparison of DRAG with state-of-the-art algorithms using the CIFAR-10 dataset under byzantine attacks with low data heterogeneity.

Through extensive testing on EMNIST and CIFAR-10 datasets against state-of-the-art algorithms, DRAG demonstrates superior performance. Furthermore, we establish DRAG's resilience to byzantine attacks that scale and reverse the direction of the local gradient.

The adaptability of DRAG opens up exciting possibilities for exploring its utilization in other scenarios. To be specific, the wireless medium could be taken into consideration to explore more practical applications; we could also search for improvements

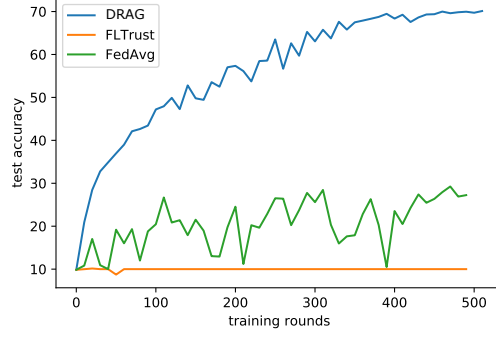


Fig. 6. Performance comparison of DRAG with state-of-the-art algorithms using the CIFAR-10 dataset under byzantine attacks with high data heterogeneity.

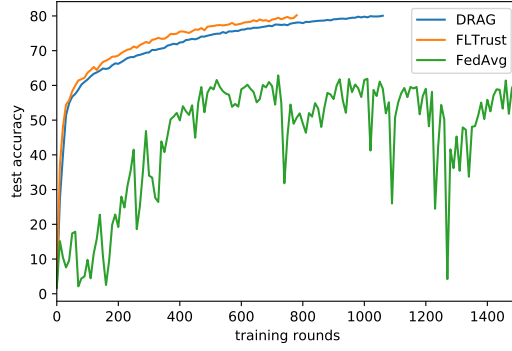


Fig. 7. Performance comparison of DRAG with state-of-the-art algorithms using the EMNIST dataset under byzantine attacks with low data heterogeneity.

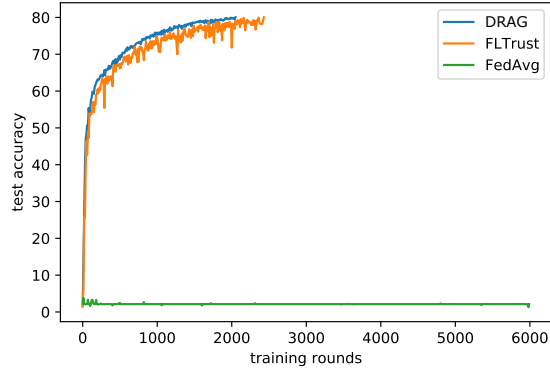


Fig. 8. Performance comparison of DRAG with state-of-the-art algorithms using the EMNIST dataset under byzantine attacks with high data heterogeneity.

of DRAG for attacks such as the label flipping attack, the Krum attack and so forth.

APPENDIX

A. Proof of Theorem 1

Due to the L -smoothness of the objective function, we have:

$$\begin{aligned} & \mathbb{E}[f(\boldsymbol{\theta}^{t+1})] \\ & \leq f(\boldsymbol{\theta}^t) + \langle \nabla f(\boldsymbol{\theta}^t), \mathbb{E}[\boldsymbol{\theta}^{t+1} - \boldsymbol{\theta}^t] \rangle + \frac{L}{2} \mathbb{E}[\|\boldsymbol{\theta}^{t+1} - \boldsymbol{\theta}^t\|^2] \end{aligned}$$

$$\begin{aligned}
&= f(\boldsymbol{\theta}^t) + \langle \nabla f(\boldsymbol{\theta}^t), \mathbb{E}[\Delta^t + a_1 - a_1] \rangle + \frac{L}{2} \mathbb{E}[\|\Delta^t\|^2] \\
&= f(\boldsymbol{\theta}^t) - (1-c)\eta U \|\nabla f(\boldsymbol{\theta}^t)\|^2 + T_1 + T_2.
\end{aligned} \tag{20}$$

where we have defined the variable $a_1 = (1-c)\eta U \nabla f(\boldsymbol{\theta}^t)$, $T_1 = \mathbb{E}[\|\Delta^t\|^2]$, and $T_2 = \langle \nabla f(\boldsymbol{\theta}^t), \mathbb{E}[\Delta^t + a_1] \rangle$.

Next, the terms T_1 and T_2 will be bounded separately. First, with T_1 we have:

$$\begin{aligned}
T_1 &\stackrel{(a1)}{=} \mathbb{E} \left[\left\| \frac{1}{S} \sum_{m \in \mathcal{S}^t} \left((1-\lambda_m^t) \mathbf{g}_m^t + \frac{\lambda_m^t \|\mathbf{g}_m^t\|}{\|\mathbf{r}^t\|} \mathbf{r}^t \right) \right\|^2 \right] \\
&\stackrel{(a2)}{\leq} \mathbb{E} \left[\left(\frac{1}{S} \sum_{m \in \mathcal{S}^t} \left((1-\lambda_m^t) \|\mathbf{g}_m^t\| + \frac{\lambda_m^t \|\mathbf{g}_m^t\|}{\|\mathbf{r}^t\|} \|\mathbf{r}^t\| \right) \right)^2 \right] \\
&\stackrel{(a3)}{=} \frac{1}{S^2} \mathbb{E} \left[\left(\sum_{m \in \mathcal{S}^t} \|\mathbf{g}_m^t\| \right)^2 \right] \\
&\stackrel{(a4)}{=} \frac{\eta^2}{S^2 B^2} \left(\sum_{m \in \mathcal{S}^t} \mathbb{E} \left[\left\| \sum_{u=0}^{U-1} \sum_{b=1}^B \nabla F(\boldsymbol{\theta}_m^{t,u}; z_{m,b}^{t,u}) \right\|^2 \right] \right) \\
&\stackrel{(a5)}{\leq} \frac{\eta^2}{S B^2} \sum_{m \in \mathcal{S}^t} \mathbb{E} \left[\left\| \sum_{u=0}^{U-1} \sum_{b=1}^B \nabla F(\boldsymbol{\theta}_m^{t,u}; z_{m,b}^{t,u}) \right\|^2 \right] \\
&\stackrel{(a6)}{=} \frac{\eta^2}{S B^2} \sum_{m \in \mathcal{S}^t} \mathbb{E} \left[\left\| \sum_{u=0}^{U-1} \sum_{b=1}^B a_2 \right\|^2 \right] \\
&\quad + \frac{\eta^2}{S} \sum_{m \in \mathcal{S}^t} \mathbb{E} \left[\left\| \sum_{u=0}^{U-1} \nabla F_m(\boldsymbol{\theta}_m^{t,u}) \right\|^2 \right] \\
&\stackrel{(a7)}{=} \frac{\eta^2 U \sigma_L^2}{B} + \frac{\eta^2}{M} \sum_{m \in \mathcal{M}} \mathbb{E} \left[\left\| \sum_{u=0}^{U-1} \nabla F_m(\boldsymbol{\theta}_m^{t,u}) \right\|^2 \right]
\end{aligned} \tag{21}$$

where (a1) is due to the definition of Δ^t ; (a2) comes from triangle inequality, i.e., $\|\mathbf{a} + \mathbf{b}\| \leq \|\mathbf{a}\| + \|\mathbf{b}\|$; (a3) comes from direct computation; (a4) is due to the definition of \mathbf{g}_m^t ; (a5) is due to Cauchy-Schwartz inequality; (a6) is because of $\mathbb{E}[\|x\|^2] = \mathbb{E}[\|x - \mathbb{E}[x]\|^2 + \|\mathbb{E}[x]\|^2]$, $\mathbb{E}[\nabla F_m(\boldsymbol{\theta}_m^{j,u}; z_{m,b}^{j,u})] = \nabla F_m(\boldsymbol{\theta}_m^{j,u})$ and the definition of variable $a_2 = \nabla F_m(\boldsymbol{\theta}_m^{t,u}; z_{m,b}^{t,u}) - \nabla F_m(\boldsymbol{\theta}_m^{t,u})$, and (a7) is due to the fact that $\mathbb{E}[\|x_1 + \dots + x_n\|^2] = \mathbb{E}[\|x_1\|^2 + \dots + \|x_n\|^2]$ if x_i 's are independent with zero mean, together with the fact that the probability of each worker being selected without replacement is $\frac{S}{M}$.

For the term T_2 , we have:

$$\begin{aligned}
T_2 &\stackrel{(b1)}{=} \left\langle \nabla f(\boldsymbol{\theta}^t), \mathbb{E} \left[(1-c) \mathbf{g}^t + \frac{c}{S} \sum_{m \in \mathcal{S}^t} \frac{\langle \mathbf{g}_m^t, \mathbf{r}^t \rangle}{\|\mathbf{g}_m^t\| \|\mathbf{r}^t\|} \mathbf{g}_m^t \right. \right. \\
&\quad \left. \left. + \frac{c}{S} \sum_{m \in \mathcal{S}^t} \frac{\|\mathbf{g}_m^t\| \|\mathbf{r}^t\| - \langle \mathbf{g}_m^t, \mathbf{r}^t \rangle}{\|\mathbf{r}^t\|^2} \mathbf{r}^t + (1-c)\eta U \nabla f(\boldsymbol{\theta}^t) \right] \right\rangle \\
&\stackrel{(b2)}{=} \underbrace{\left\langle \nabla f(\boldsymbol{\theta}^t), \mathbb{E}[(1-c) \mathbf{g}^t + a_1] \right\rangle}_{T_{2,1}} \\
&\quad + \underbrace{\left\langle \nabla f(\boldsymbol{\theta}^t), \mathbb{E} \left[\frac{c}{M} \sum_{m \in \mathcal{S}^t} \frac{\langle \mathbf{g}_m^t, \mathbf{r}^t \rangle}{\|\mathbf{g}_m^t\| \|\mathbf{r}^t\|} \mathbf{g}_m^t \right] \right\rangle}_{T_{2,2}} \\
&\quad + \underbrace{\left\langle \nabla f(\boldsymbol{\theta}^t), \mathbb{E} \left[\frac{c}{M} \sum_{m \in \mathcal{S}^t} \frac{\|\mathbf{g}_m^t\| \|\mathbf{r}^t\| - \langle \mathbf{g}_m^t, \mathbf{r}^t \rangle}{\|\mathbf{r}^t\|^2} \mathbf{r}^t \right] \right\rangle}_{T_{2,3}},
\end{aligned} \tag{22}$$

where (b1) comes from the definition of Δ^t and (b2) comes from decomposition, where $\mathbf{g}^t = \frac{1}{S} \sum_{m \in S^t} \mathbf{g}_m^t$. The three terms $T_{2,1}$, $T_{2,2}$ and $T_{2,3}$ are then bounded separately.

For the term $T_{2,1}$, we have:

$$\begin{aligned}
T_{2,1} &= \langle \nabla f(\boldsymbol{\theta}^t), \mathbb{E}[(1-c)\mathbf{g}^t + a_1] \rangle \\
&\stackrel{(c1)}{=} \langle \nabla f(\boldsymbol{\theta}^t), \mathbb{E}[(1-c)\bar{\mathbf{g}}^t + a_1] \rangle \\
&\stackrel{(c2)}{=} \left\langle \nabla f(\boldsymbol{\theta}^t), \mathbb{E} \left[- (1-c) \frac{1}{M} \sum_{m=1}^M \sum_{u=0}^{U-1} \eta \nabla F_m(\boldsymbol{\theta}_m^{t,u}) \right. \right. \\
&\quad \left. \left. + (1-c)\eta U \frac{1}{M} \sum_{m=1}^M \nabla F_m(\boldsymbol{\theta}^t) \right] \right\rangle \\
&\stackrel{(c3)}{=} \left\langle \sqrt{\eta U (1-c)} \nabla f(\boldsymbol{\theta}^t), -\frac{\sqrt{\eta(1-c)}}{M\sqrt{U}} \mathbb{E} \left[\sum_{m=1}^M \sum_{u=0}^{U-1} a_3 \right] \right\rangle \\
&\stackrel{(c4)}{\leq} a_4 + \frac{(1-c)\eta}{2UM^2} \mathbb{E} \left[\left\| \sum_{m=1}^M \sum_{u=0}^{U-1} a_3 \right\|^2 \right] \\
&\stackrel{(c5)}{\leq} a_4 + \frac{(1-c)\eta}{2M} \sum_{m=1}^M \sum_{u=0}^{U-1} \mathbb{E} [\|a_3\|^2] \\
&\stackrel{(c6)}{\leq} a_4 + \frac{(1-c)\eta L^2}{2M} \sum_{m=1}^M \sum_{u=0}^{U-1} \mathbb{E} [\|\boldsymbol{\theta}_m^{t,u} - \boldsymbol{\theta}^t\|^2], \tag{23}
\end{aligned}$$

where (c1) is due to the fact that the sampling distribution is identical at every round; (c2) comes from the definition of $\bar{\mathbf{g}}^t = \frac{1}{M} \sum_{m \in \mathcal{M}} \mathbf{g}_m^t$ and $f(\boldsymbol{\theta}^t)$; (c3) comes from direct computation and the defined variable $a_3 = \nabla F_m(\boldsymbol{\theta}_m^{t,u}) - \nabla F_m(\boldsymbol{\theta}^t)$; (c4) follows from $\langle \mathbf{x}, \mathbf{y} \rangle \leq \frac{1}{2}[\|\mathbf{x}\|^2 + \|\mathbf{y}\|^2]$ and the defined variable $a_4 = \frac{(1-c)\eta U}{2} \|\nabla f(\boldsymbol{\theta}^t)\|^2$; (c5) uses Cauchy-Schwartz inequality; and (c6) is due to the L -smoothness assumption.

Similarly, by following the bounding operation of $T_{2,1}$, we can have the following two inequalities

$$T_{2,2} \leq a_4 + \frac{c\eta}{SU} \sum_{m \in S^t} \mathbb{E} \left[\left\| \sum_{u=0}^{U-1} \nabla F_m(\boldsymbol{\theta}_m^{t,u}) \right\|^2 \right], \tag{24}$$

$$T_{2,3} \leq a_4 + \frac{4c\eta\sigma_L^2}{B} + \frac{4c\eta}{MU} \sum_{m \in \mathcal{M}} \mathbb{E} \left[\left\| \sum_{u=0}^{U-1} \nabla F_m(\boldsymbol{\theta}_m^{t,u}) \right\|^2 \right], \tag{25}$$

We continue to bound the following term:

$$\begin{aligned}
&\mathbb{E} \left[\left\| \sum_{u=0}^{U-1} \nabla F_m(\boldsymbol{\theta}_m^{t,u}) \right\|^2 \right] \\
&= \mathbb{E} \left[\left\| \sum_{u=0}^{U-1} (a_3 + \nabla F_m(\boldsymbol{\theta}^t) - \nabla f(\boldsymbol{\theta}^t) + \nabla f(\boldsymbol{\theta}^t)) \right\|^2 \right] \\
&\stackrel{(f1)}{\leq} 3UL^2 \sum_{u=0}^{U-1} \mathbb{E} [\|\boldsymbol{\theta}_m^{t,u} - \boldsymbol{\theta}^t\|^2] + 3U^2\sigma_G^2 + 3U^2\|\nabla f(\boldsymbol{\theta}^t)\|^2 \\
&\stackrel{(f2)}{=} C_1\|\nabla f(\boldsymbol{\theta}^t)\|^2 + C_2, \tag{26}
\end{aligned}$$

where (f1) is due to Cauchy-Schwartz inequality; (f2) is from [42, Lemma 3], which proves the inequality

$$\mathbb{E} [\|\boldsymbol{\theta}_m^{t,u} - \boldsymbol{\theta}^t\|^2] \leq 5U\eta^2(\sigma_L^2 + 6U\sigma_G^2) + 30U^2\eta^2\|\nabla f(\boldsymbol{\theta}^t)\|^2;$$

and we have the definitions with $C_1 = 90U^4L^2\eta^2 + 3U^2$ and $C_2 = 15U^3L^2\eta^2(\sigma_L^2 + 6U\sigma_G^2) + 3U^2\sigma_G^2$.

Hence, we can bound T_2 by using (23), (24) and (25). Together with (21), we have

$$\mathbb{E}[f(\boldsymbol{\theta}^{t+1})]$$

$$\leq f(\boldsymbol{\theta}^t) - \eta U \left(\frac{1-3c}{2} - \left(\frac{5c}{U} + \frac{\eta L}{2} \right) (90U^3 L^2 \eta^2 + 3U) - \frac{30(1-c)L^2 U^2 \eta^2}{2} \right) \|\nabla f(\boldsymbol{\theta}^t)\|^2 + C_3, \quad (27)$$

where $C_3 = \frac{4c\eta\sigma_L^2}{B} + \frac{\eta^2 U \sigma_L^2 L}{2B} + \left(\frac{5c\eta}{U} + \frac{\eta^2 L}{2} \right) C_2 + \frac{5(1-c)\eta^3 L^2 U^2}{2} (\sigma_L^2 + 6U\sigma_G^2)$.

Rearranging and summing from $t = 0, \dots, T-1$, we have:

$$\frac{1}{T} \sum_{t=0}^{T-1} \|\nabla f(\boldsymbol{\theta}^t)\|^2 \leq \frac{f(\boldsymbol{\theta}^0) - f^*}{\gamma \eta U T} + V, \quad (28)$$

where there exists a constant γ satisfying $\frac{1-3c}{2} - \left(\frac{5c}{U^2} + \frac{\eta L}{2U} \right) C_1 - \frac{30(1-c)L^2 U^2 \eta^2}{2} > \gamma > 0$ and $V = \frac{C_3}{\gamma U \eta}$. The proof is then complete.

REFERENCES

- [1] J. Dean *et al.*, "Large scale distributed deep networks," in *Proc. of Neural Information Processing Systems*, Dec. 2012, pp. 1223–1231.
- [2] V. Smith, C.-K. Chiang, M. Sanjabi, and A. Talwalkar, "Federated multi-task learning," in *Proc. of Neural Information Processing Systems*, Dec. 2017, p. 4427–4437.
- [3] W. Y. B. Lim, N. C. Luong, D. T. Hoang, Y. Jiao, Y.-C. Liang, Q. Yang, D. Niyato, and C. Miao, "Federated learning in mobile edge networks: A comprehensive survey," *IEEE Commun. Surveys Tuts.*, vol. 22, no. 3, pp. 2031–2063, 2020.
- [4] Q. Yang, Y. Liu, T. Chen, and Y. Tong, "Federated machine learning: Concept and applications," *ACM Trans. Intell. Syst. Technol.*, vol. 10, no. 2, pp. 1–19, 2019.
- [5] X. Lian, C. Zhang, H. Zhang, C. J. Hsieh, W. Zhang, and J. Liu, "Can decentralized algorithms outperform centralized algorithms? A case study for decentralized parallel stochastic gradient descent," in *Proc. Neural Inf. Process. Syst.*, vol. 30, 2017, pp. 5336–5346.
- [6] M. Li, D. G. Andersen, J. W. Park, A. J. Smola, A. Ahmed, V. Josifovski, J. Long, E. J. Shekita, and B.-Y. Su, "Scaling distributed machine learning with the parameter server," in *Proc. Symp. Oper. Syst. Design Implement.*, 2014, pp. 583–598.
- [7] S. Gupta, W. Zhang, and F. Wang, "Model accuracy and runtime tradeoff in distributed deep learning: A systematic study," in *Proc. IEEE Int. Conf. Data Mining*, 2016, pp. 171–180.
- [8] S. Zhang, A. E. Choromanska, and Y. LeCun, "Deep learning with elastic averaging SGD," in *Proc. Neural Inf. Process. Syst.*, vol. 28, 2015.
- [9] D. Alistarh, D. Grubic, J. Li, R. Tomioka, and M. Vojnovic, "QSGD: Communication-efficient sgd via gradient quantization and encoding," in *Proc. Neural Inf. Process. Syst.*, vol. 30, 2017.
- [10] M. Zinkevich, M. Weimer, A. J. Smola, and L. Li, "Parallelized stochastic gradient descent," in *Proc. Neural Inf. Process. Syst.*, vol. 23, 2010, pp. 2595–2603.
- [11] H. B. McMahan, E. Moore, D. Ramage, S. Hampson, and B. Arcas, "Communication-efficient learning of deep networks from decentralized data," in *Proc. Artif. Intell. and Statist.*, 2017, pp. 1273–1282.
- [12] D. Zhou, J. Chen, Y. Cao, Y. Tang, Z. Yang, and Q. Gu, "On the convergence of adaptive gradient methods for nonconvex optimization," *arXiv preprint arXiv:1808.05671*, 2018.
- [13] B. Woodworth, J. Wang, B. McMahan, and N. Srebro, "Graph oracle models, lower bounds, and gaps for parallel stochastic optimization," in *Proc. Neural Inf. Process. Syst.*, vol. 31, 2018, pp. 8505–8515.
- [14] J. Wang and G. Joshi, "Cooperative SGD: A unified framework for the design and analysis of communication-efficient SGD algorithms," in *Proc. ICML Workshop Coding Theory Mach. Learn.*, 2019.
- [15] A. Khaled, K. Mishchenko, and P. Richtárik, "Tighter theory for local sgd on identical and heterogeneous data," in *International Conference on Artificial Intelligence and Statistics*. PMLR, 2020, pp. 4519–4529.
- [16] Y. Zhao, M. Li, L. Lai, N. Suda, D. Civin, and V. Chandra, "Federated learning with non-iid data," *arXiv preprint arXiv:1806.00582*, 2018.
- [17] S. P. Karimireddy, S. Kale, M. Mohri, S. Reddi, S. Stich, and A. T. Suresh, "Scaffold: Stochastic controlled averaging for federated learning," in *International Conference on Machine Learning*. PMLR, 2020, pp. 5132–5143.
- [18] F. Varno, M. Saghayei, L. Rafiee Sevyeri, S. Gupta, S. Matwin, and M. Havaei, "Adabest: Minimizing client drift in federated learning via adaptive bias estimation," in *Proc. Eur. Conf. Comput. Vision*, 2022, pp. 710–726.
- [19] J. So, B. Güler, and A. S. Avestimehr, "Byzantine-resilient secure federated learning," *IEEE Journal on Selected Areas in Communications*, vol. 39, no. 7, pp. 2168–2181, 2020.
- [20] X. Cao, M. Fang, J. Liu, and N. Z. Gong, "Fltrust: Byzantine-robust federated learning via trust bootstrapping," *arXiv preprint arXiv:2012.13995*, 2020.
- [21] E. Bagdasaryan, A. Veit, Y. Hua, D. Estrin, and V. Shmatikov, "How to backdoor federated learning," in *International Conference on Artificial Intelligence and Statistics*, 2020, pp. 2938–2948.
- [22] S. Prakash and A. S. Avestimehr, "Mitigating byzantine attacks in federated learning," *arXiv preprint arXiv:2010.07541*, 2020.
- [23] A. Defazio, F. Bach, and S. Lacoste-Julien, "Saga: A fast incremental gradient method with support for non-strongly convex composite objectives," in *Advances in Neural Information Processing Systems*, vol. 27, 2014.
- [24] R. Johnson and T. Zhang, "Accelerating stochastic gradient descent using predictive variance reduction," in *Advances in Neural Information Processing Systems*, vol. 26, 2013.
- [25] X. Liang, S. Shen, J. Liu, Z. Pan, E. Chen, and Y. Cheng, "Variance reduced local SGD with lower communication complexity," *arXiv preprint arXiv:1912.12844*, 2019.
- [26] T. Li, A. K. Sahu, M. Zaheer, M. Sanjabi, A. Talwalkar, and V. Smithy, "FedDane: A federated newton-type method," in *Proc. Asilomar Conf. Signals, Syst., and Comput.*, 2019, pp. 1227–1231.
- [27] R. Pathak and M. J. Wainwright, "Fedsplit: An algorithmic framework for fast federated optimization," in *Proc. Neural Inf. Process. Syst.*, vol. 33, 2020, pp. 7057–7066.
- [28] J. Konečný, H. B. McMahan, D. Ramage, and P. Richtárik, "Federated optimization: Distributed machine learning for on-device intelligence," *arXiv preprint arXiv:1610.02527*, 2016.
- [29] S. P. Karimireddy, M. Jaggi, S. Kale, M. Mohri, S. J. Reddi, S. U. Stich, and A. T. Suresh, "MIME: Mimicking centralized stochastic algorithms in federated learning," *arXiv preprint arXiv:2008.03606*, 2020.

- [30] D. A. E. Acar, Y. Zhao, R. M. Navarro, M. Mattina, P. N. Whatmough, and V. Saligrama, "Federated learning based on dynamic regularization," *arXiv preprint arXiv:2111.04263*, 2021.
- [31] T. Li, A. K. Sahu, M. Zaheer, M. Sanjabi, A. Talwalkar, and V. Smith, "Federated optimization in heterogeneous networks," in *Proc. of Mach. Learn. and Syst.*, vol. 2, 2020, pp. 429–450.
- [32] L. Gao, H. Fu, L. Li, Y. Chen, M. Xu, and C.-Z. Xu, "FedDC: Federated learning with non-iid data via local drift decoupling and correction," in *Proc. Conf. Comput. Vision and Pattern Recognit.*, 2022, pp. 10 112–10 121.
- [33] M. Fang, X. Cao, J. Jia, and N. Gong, "Local model poisoning attacks to {Byzantine-Robust} federated learning," in *29th USENIX Security Symposium (USENIX Security 20)*, 2020, pp. 1605–1622.
- [34] P. Blanchard, E. M. El Mhamdi, R. Guerraoui, and J. Stainer, "Machine learning with adversaries: Byzantine tolerant gradient descent," *Advances in Neural Information Processing Systems*, vol. 30, 2017.
- [35] D. Yin, Y. Chen, R. Kannan, and P. Bartlett, "Byzantine-robust distributed learning: Towards optimal statistical rates," in *International Conference on Machine Learning*, 2018, pp. 5650–5659.
- [36] H. Yang, M. Fang, and J. Liu, "Achieving linear speedup with partial worker participation in non-IID federated learning," in *Proc. Int. Conf. on Learning Representations*, 2020.
- [37] F. Haddadpour, M. M. Kamani, M. Mahdavi, and V. R. Cadambe, "Local SGD with periodic averaging: Tighter analysis and adaptive synchronization," in *Proc. Neural Inf. Process. Syst.*, vol. 32, 2019, pp. 11 082–11 094.
- [38] H. Yu, S. Yang, and S. Zhu, "Parallel restarted SGD with faster convergence and less communication: Demystifying why model averaging works for deep learning," in *Proc. AAAI Conf. Artif. Intell.*, vol. 33, 2019, pp. 5693–5700.
- [39] G. Cohen, S. Afshar, J. Tapson, and A. Van Schaik, "EMNIST: Extending MNIST to handwritten letters," in *2017 International Joint Conference on Neural Networks (IJCNN)*, 2017, pp. 2921–2926.
- [40] A. Krizhevsky, G. Hinton *et al.*, "Learning multiple layers of features from tiny images," 2009.
- [41] Q. Li, Y. Diao, Q. Chen, and B. He, "Federated learning on non-iid data silos: An experimental study," *arXiv preprint arXiv:2102.02079*, 2021.
- [42] S. J. Reddi, Z. Charles, M. Zaheer, Z. Garrett, K. Rush, J. Konečný, S. Kumar, and H. B. McMahan, "Adaptive federated optimization," in *Proc. ICLR*, 2020.